Journal of Achievements in Materials and Manufacturing Engineering

VOLUME 20
ISSUES 1-2
January-February
2007

The effect of thermal properties and weld efficiency on residual stresses in welding

E. Armentani*, R. Esposito, R. Sepe
Department of Industrial Design and Management,
University of Naples Federico II, P.le Tecchio 80, 80125 Naples, Italy
* Corresponding author: E-mail address: enrico.armentani@unina.it

Received 18.10.2006; accepted in revised form 15.11.2006

Analysis and modelling

ABSTRACT

Purpose: A parametric model is adopted and the technique of element "birth and death" is used to estimate the effect of thermal properties and weld efficiency on residual stresses in butt weld joints.
Design/methodology/approach: Residual stresses and distortions on butt welded joints are numerically evaluated by means of finite element method. The FE analysis allows to highlight and evaluate the stress field and its gradient around the fusion zone of welded joints, higher than any other located in the surrounding area.
Findings: The main conclusion is the significant effect of varying the value of the conductivity on residual stresses.
Practical implications: Several experimental destructive and non destructive techniques for directly measuring residual stress have been developed. However, the application of these methods in practice is usually limited by either cost or accuracy. Numerical simulation based on finite element techniques, therefore, offers a comprehensive solution for the prediction of residual stress and strain as well as welding distortion in complex welded structures.
Originality/value: In this study it is shown that the technique of element "birth and death" can be usefully applied to welding process in order to take in account the effect of the thermal properties of materials.
Keywords: Numerical techniques; Residual stresses; Welding; Thermo-mechanical analysis

1. Introduction

Fusion welding is a joining process extensively used in construction, ship building, steel bridges, pressure vessels, etc. The advantages of welding, as a joining process, include high joint efficiency, simple set up, flexibility and low fabrication costs. However when structures are manufactured by welding, a non-uniform temperature distribution is produced. This distribution initially causes a rapid thermal expansion followed by a thermal contraction in the weld and surrounding areas, thus generating inhomogeneous plastic deformation and residual stresses in the weldment when it is cooled.

As it is well known, the residual stresses have a strong influence on weld deformation, fatigue strength, fracture toughness and buckling strength. Thus, it is important to evaluate the residual stresses due to welding. However evaluating residual stresses associated to a welded joint is extremely complicated. Difficulty in determining these stresses is emphasized by the thermal transient, by the variation of the thermal and mechanical properties of the material with the temperature and by the non linear heat losses.

Several experimental destructive and non destructive techniques for directly measuring residual stress have been developed. These techniques include X-ray diffraction method [1], neutron diffraction method [2,3], layer-removal method, sectioning method, ultrasonic and magnetic methods, and hole drilling method [4,5]. However , the application of these methods in practice is usually limited by either cost or accuracy.

Numerical simulation based on finite element methods, therefore, offers a comprehensive solution for the prediction of residual stress and strain as well as welding distortion in welded structures [6-14].

In the present paper, a parametric model is adopted and the elements "birth and death" are used in single-pass butt welded joint in order to simulate the weld filler variation with time. The effect of thermal properties and weld efficiency on transient temperatures during welding was studied and the residual stresses after welding were determined by the finite element method. A fully coupled thermal–mechanical two-dimensional analysis was performed with the commercial software program ANSYS and heat flow was evaluated by a non-linear transient analysis.

2. Analysis model

A theoretical evaluation of welded induced residual stresses and strains can be achieved in two steps: (a) heat flow analysis; (b) residual stress and deformation analysis.

2.1. Thermal and mechanical model

The transient temperature distribution T of the welded plate is a function of time t and coordinates x, y, z, and the balance relation of heat flow of a volume bounded by an arbitrary surface S is given by the following equation:

$$\frac{\partial}{\partial x}\left(k_x \frac{\partial T}{\partial x}\right)+\frac{\partial}{\partial y}\left(k_y \frac{\partial T}{\partial y}\right)+\frac{\partial}{\partial z}\left(k_z \frac{\partial T}{\partial z}\right)+\dot{q} = \rho C \frac{\partial T}{\partial t} \quad (1)$$

where ρ, C, and k_i are the density, specific heat capacity and thermal conductivity, respectively, in i direction of the plate material and they depending on the temperature, whereas $\dot{q}$ is the rate of internal heat generation. Eq. (1) is a differential equation governing heat conduction in a solid body. The initial and boundary conditions of the problem are:

$$T(x,y,z,t=0) = T_0(x,y,z) \quad (2)$$

$$k \cdot \left(\frac{\partial T}{\partial x}+\frac{\partial T}{\partial y}+\frac{\partial T}{\partial z}\right)+q_s+h_c(T-T_\infty)+h_r(T-T_r)=0 \quad (3)$$

where k is thermal conductivity in the normal direction, h_c and h_r are convection and emissive coefficients, respectively, for all surfaces of the plate, q_s is the heat flux at the boundary S of the body, T_∞ is the room temperature and T_r is the temperature of the emissive body. In this study the flux losses due to the radiation are not considered. In addition, a latent heat of fusion is taken into account to consider the phase transformation.

The temperature history during the thermal analysis at the nodes of the FE mesh is calculated and saved, for the mechanical analysis. During the structural analysis, these temperature histories are used as thermal loading to produce the residual stress field. In this way thermal strains and stresses can be calculated at each time increment. In thermo-mechanical analysis, the plastic deformation of materials is assumed by considering the Mises yield criterion and isotropic strain hardening rule.

2.2. Considered parameters

In this study the effect of thermal properties and weld efficiency on residual stresses are taken in account. In fact thermal and mechanical properties of materials depend on temperature. Particularly for steel, the specific heat capacity, C, varies strongly with temperature [15], whereas it does not vary much with steel type. On the contrary the thermal conductivity k for steels varies widely in function of the type of employed material. Fig. 1 shows the curves that define the variation of thermal conductivity k with temperature. Each curve is calculated starting from the conductivity k_0 at 293 K.

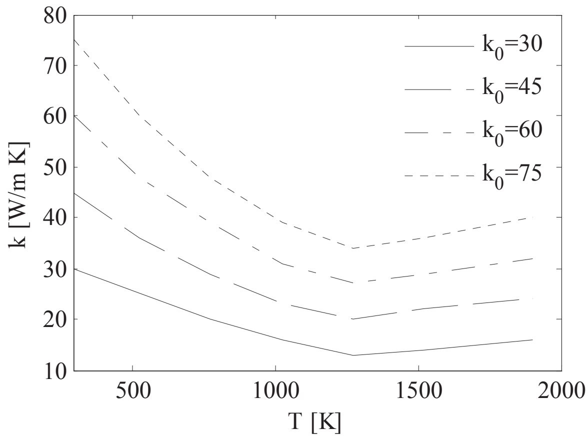

Fig. 1. Thermal conductivity k

Typically k_0 varies from about 15 W/mK for alloy steels to about 75 W/mK for low carbon steels. A set of four values of k_0 (30, 45, 60 and 75 W/mK) is used in this study. Instead specific heat capacity has been considered equal for all steels and its curve is reported in [15]. The values of the arc efficiency coefficient, η, depend on different welding and they vary from 20 % for GTAW to 95% for SAW processes. Three values of η (40, 60 and 80%) are taken into account. Only one parameter was varied at a time and, when each parameter varied, the other was set at standard value, where the standard values of k_0 and η were 45 $Wm^{-1}K$ and 80% respectively.

2.3. Butt joint

Fig. 2 shows the geometry of the welded joint considered in this study. The plates are 10 mm thick and the joint is 300 mm long in the welding direction; they are joined by a single-pass butt weld. The total effective heat generation rate input $\dot{q} = \eta IV$ is assumed to be 1200, 1800 and 3000 W that correspond to the following welding parameters: welding current I = 100 A, welding voltage V = 30 V, and η = 40, 60 and 80% respectively.

The welding velocity v = 5 mm s^{-1} is assumed for all cases studied. The convective heat coefficient on the surfaces was estimated to be 15 W/m^2K according to [15]. The material mechanical properties (Young modulus, yield stress, thermal expansion coefficient and Poisson modulus) are taken from [15] and these also vary according to the temperature history.

This work develops a two-dimensional symmetrical plane stress model (assuming zero out-of-plane stresses) to estimate the residual stresses. The model employs two dimensional four-node plane elements including the finite element meshes for the butt welded joint.

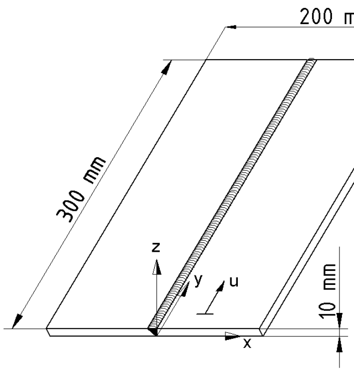

Fig. 2. Geometry of the butt welded joint

2.4. Element birth and death

In this study the technique of element birth and death is adopted; this procedure can be used to simulate the process of filler metal addition. All elements must be created, including those weld fillers to be born in later stages of the analysis. To achieve the "element death" effect the elements are not actually removed. These are deactivated by multiplying their stiffness by a severe reduction factor. Likewise, when elements are ''born'', they are not actually added to the model, but are simply reactivated. When an element is reactivated, its stiffness, mass, element loads, etc. return to their full original values.

3. Results

3.1. Temperature distribution

Fig. 3 shows the temperature distribution along longitudinal direction during welding processes at welding time of 29 s, at transverse distance $x = 6{,}8$ mm. The centre of the welding arc at this time is at the position of $x = 0$ mm and $y = 145$ mm. It shows that when k_0 increases the temperature at points near the weldment decreases while those related to the points in front of the heat source are higher.

Fig. 4 shows the temperature distribution along transversal direction when the torch is positioned at $y = 145$ mm. It shows that the temperature in fusion zone (FZ) ($x < 3{,}2$ mm) is substantially higher for lower values of k_0. Moreover for high values of k_0 the temperature at the points that are further away from FZ increase in consequence of higher heat flows through the plate.

From Fig. 5 it can be noted that the variations of temperature versus efficiency η have the same tendency for all three values of η. In fact changing η is equivalent to change the effective heat generation rate.

3.2. Residual stresses distribution

Residual stresses are evaluated using the same mesh that was used for calculating the temperatures. Normal stresses parallel to the direction of the weld are called longitudinal residual stresses and denoted by σ_y. The longitudinal residual stresses develop from longitudinal expansion and contraction during the welding sequence.

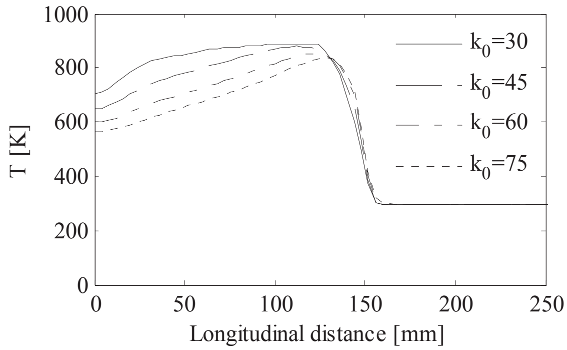

Fig. 3. Longitudinal temperature distribution at time of 29 s for several conductivity coefficient

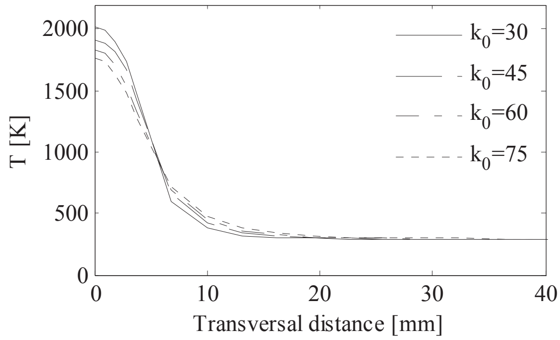

Fig. 4. Transversal temperature distribution at time of 29 s for several conductivity coefficient

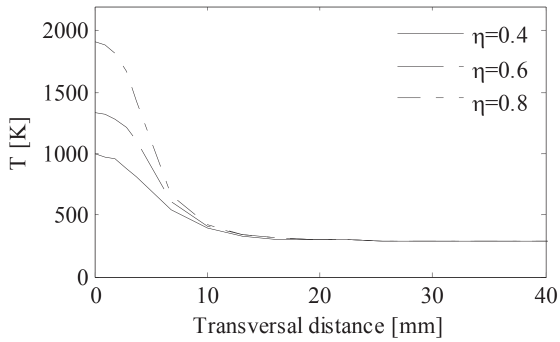

Fig. 5. Transversal temperature distribution at time of 29 s for several efficiency

Fig. 6 shows the distribution of the residual stresses σ_y along the x direction in the midsection ($y = 150$ mm).

The variations of residual stresses versus conductivity k have the same tendency for all values of k evaluated. It can be noted that with increasing of k_0, high tensile residual stresses, present in regions near the welding line, due to a resistance contraction of the material as cooling begins, decrease. Moreover it appears that for increasing the conductivity from 30 W/mK to 75 W/mK the residual stresses in the weldment are reduced of about 15%.

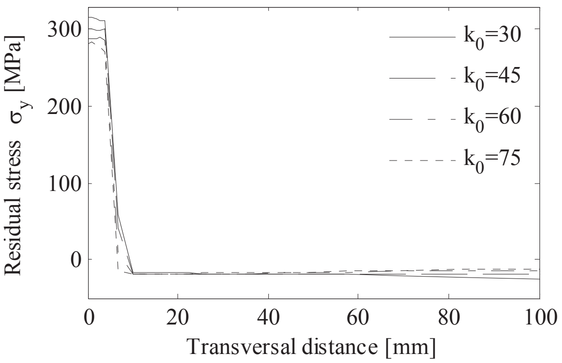

Fig. 6. Longitudinal stress distribution at midsection (y =150 mm) for several conductivity coefficient

Normal stresses orthogonal to the direction of the weld are known as transverse residual stresses, denoted by σ_x. Tensile residual stresses are present in regions near the welding line, then decrease close to zero as the distance from the welding line increases. Fig. 7 shows the distribution of the residual stress σ_x along the x direction in the midsection (y = 150 mm). Also in this case increasing the conductivity from 30 W/mK to 75 W/mK decreasing the residual stresses in the weldment.

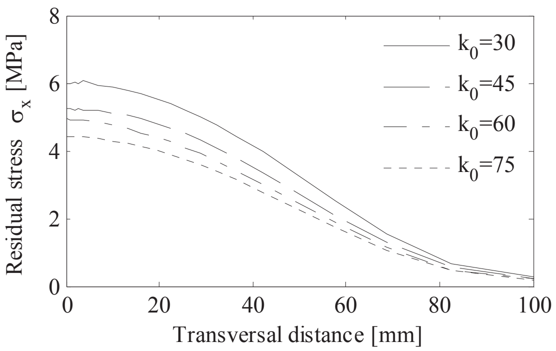

Fig. 7. Transversal stress distribution at midsection (y = 150 mm) for several conductivity coefficient

4. Conclusions

To evaluate residual stresses in a welding process, 2D nonlinear thermal and thermo-mechanical analyses are achieved using FE analyses. Moreover the technique of element birth and death is used to simulate the welding filler varying with time in weldments. The main results and conclusions are summarized as follows: 1) transient temperature distribution in a welded joint is highly affected by thermal conductivity; 2) the variations of temperature versus efficiency have the same tendency for all three evaluated values; 3) large tensile longitudinal residual stresses are present near the welding bead, and the magnitude of these stresses are reduced of about 15% when conductivity increasing from 30 W/mK to 75 W/mK; 4) low transverse residual stresses are produced near the weldments, but they are affected by thermal conductivity change.

References

[1] S. Murugan, S.K. Rai, P.V. Kumar, T. Jayakumar, B. Raj, M.S.C. Bose, Temperature distribution and residual stresses due to multipass welding in type 304 stainless steel and low carbon steel weld pads, International Journal of Pressure and Piping, 78 (2001) 307-317.

[2] M.J. Park, H.N. Yang, D.Y. Jang, J.S. Kim, T.E. Jin, Residual stress measurement on welded specimen by neutron diffraction, Journal of Materials Processing Technology 155–156 (2004) 1171–1177.

[3] R.A. Owen, R.V. Preston, P.J. Withers, H.R. Shercliff, P.J. Webster, Neutron and synchrotron measurements of residual strain in TIG welded aluminum alloy 2024, Materials Science and Engineering, A346 (2003) 159-167

[4] G.S. Schajer, Measurement of non-uniform residual stresses using the hole-drilling method Part. I-II, Journal of Engineering Materials and Technology 110 (1988) 338–343.

[5] G. Roy, M. Braid, G. Shen, Application of ADINA and hole drilling method to residual stress determination in weldments, Computers and Structures, 81 (2003) 929–935.

[6] N. Siva Prasad,. T.K. Sankaranarayanan, Estimation of residual stresses in weldments using adaptive grids, Computers and Structures, 80 (6) (1996) 1037-1045.

[7] P. Mollicone, D. Camilleri, T.G.F. Gary, T. Comlekci, Simple thermo-elastic-plastic models for welding distortion simulation, Journal of Materials Processing Technology 176 (2006) 77–86.

[8] J.R. Cho, B.Y. Lee, Y.H. Moon, C.J. Van Tyne, Investigation of residual stress and post weld heat treatment of multi-pass welds by finite element method and experiments, Journal of Materials Processing Technology 155-156 (2004) 1690–1695.

[9] S.W. Wen, P. Hilton, D.C.J. Farrugia, Finite element modeling of a submerged arc welding process, Journal of Materials Processing Technology 119 (2001) 203–209 .

[10] A. Carpinteri, C. Majorana, Fully three-dimensional thermo-mechanical analysis of steel welding processes, Journal of Materials Processing Technology 53 (1995) 85–92.

[11] D. Gery, H. Long, P. Maropoulos, Effects of welding speed energy input and heat source distribution on temperature variations in butt joint welding, Journal of Materials Processing Technology 167 (2005) 393–401.

[12] X.K. Zhu, Y.J. Chao, Numerical simulation of transient temperature and residual stresses in friction stir welding of 304L stainless steel, Journal of Materials Processing Technology 146 (2004) 263–272.

[13] S.A. Tsirkas, P. Papanikos, Th. Kermanidis, Numerical simulation of the laser welding process in butt-joint specimens, Journal of Materials Processing Technology 134 (2003) 59–69.

[14] C.M. Chen, R. Kovacevic, Finite element modeling of friction stir welding – thermal and thermo-mechanical analysis, International Journal of Machine Tools & Manufacture, 43 (2003) 1319-1326.

[15] J.H. Argyris, J. Szimmat, K.J. Williams, Finite element analysis of arc welding process, In: Numerical Methods in Heat Transfer (Edited by R. W. Lewis and K. Morgan),. Wiley, New York, 3 (1985) 1-33.